ORIGINAL ARTICLE

Effect of shear and rotatory inertia on the bending vibration method without weighing specimens

Yoshitaka Kubojima[1*], Satomi Sonoda[2], Hideo Kato[1] and Masaki Harada[1]

Abstract

This study examines the effect of shear and rotatory inertia on the accuracy of the vibration method with additional mass (VAM). Bending vibration tests were performed for rectangular bars with a width of 30 mm, thicknesses ranging from 5 to 60 mm, and a length of 300 mm, small round bars with diameters in the range of 6–36 mm, and lengths of 150–300 mm, and cross beams for timber guardrails with and without a concentrated mass under a free–free condition. The estimation accuracy of the VAM and the effect of shear and rotatory inertia increased and decreased, respectively, as the length/thickness ratio of the rectangular bar and length/diameter ratio of the round bar increased. The estimation accuracy of the VAM decreased with an increase in the effect of shear and rotatory inertia, and it could be corrected. The range of the effect of shear and rotatory inertia for the sufficient estimation accuracy of the VAM was obtained.

Keywords: Bending vibration, Rotatory inertia, Shear, Specimen dimension, Vibration method with additional mass

Introduction

The vibration test is widely used because it enables Young's modulus to be measured simply, quickly, and non-destructively. Density is a necessary input for calculating the Young's modulus. Weighing specimens can be challenging for certain materials, such as each piled lumber and each cross-beam of timber guardrails. Therefore, a measuring method that does not require specimens to be weighed when measuring Young's modulus would represent a significant practical improvement.

A method for measuring mass, density, and Young's modulus without needing to weigh the specimen was developed based on a frequency equation that incorporates the effect of an additional mass attached to a wooden bar [1–6]. This method is referred to as the vibration method with additional mass (VAM) in this study. This method utilizes decreases in the resonance frequency by attaching additional mass. The ratio of the resonance frequency with the additional mass to that without it is used for the frequency equation, incorporating the effect of the concentrated mass attached on a specimen and its position. The mass ratio (concentrated mass/specimen) is subsequently calculated from the frequency equation.

To analyze the potential application of the VAM for practical purposes, a series of parameters were investigated, including the suitable mass ratio (additional mass/specimen) [7], the connection between the additional mass and specimen [7], the crossers' position for the piled lumber [8], the specimen moisture content [9], and the bending vibration generation method [10]. The VAM could perhaps be used to assess the deterioration of the cross beams of timber guardrails [11].

Although the VAM in conjunction with the bending vibration may be effective for piled lumber [12] and the cross beams of timber guardrails [11], the apparent deflection in the bending vibration consists of deflections due to shear and rotatory inertia, as well as pure bending deflection. Hence, this study aims to investigate the effect

*Correspondence: kubojima@ffpri.affrc.go.jp
[1] Forestry and Forest Products Research Institute, 1 Matsunosato, Tsukuba, Ibaraki 305-8687, Japan
Full list of author information is available at the end of the article

Kubojima *et al. J Wood Sci*   (2020) 66:51

Page 2 of 8

of shear and rotatory inertia on the estimation accuracy of the VAM.

Theory

Vibration testing method without weighing the specimen

Here, bending vibrations under free–free conditions are considered. In the case of a thin beam with constant cross section, the effect of deflections due to shear and rotatory inertia involved in the bending vibrational deflection (hereafter, SR effect) is negligible, and the Euler–Bernoulli elementary theory of bending can be applied to the bending vibration.

The resonance frequency, represented by f_{n0} (n: resonance mode number, 0: value without the additional mass), is expressed as follows:

$$f_{n0} = \frac{1}{2\pi} \left(\frac{m_{n0}}{l} \right)^2 \sqrt{\frac{EI}{\rho A}}, \tag{1}$$

where l, E, ρ, I, and A are the specimen length, Young's modulus, density, the second moment of area, and the cross-sectional area, respectively. m_{n0} is a constant that depends on the end conditions and is expressed as follows:

$$m_{10} = 4.730, m_{20} = 7.853, m_{30} = 10.996, m_{n0} = \frac{1}{2}(2n+1)\pi(n > 3). \tag{2}$$

The resonance frequency is decreased experimentally by attaching the additional mass, while the dimensions, density, and Young's modulus are not altered. Hence, it can be said that m_{n0} changes to m_n. The resonance frequency after attaching the additional mass is expressed as follows:
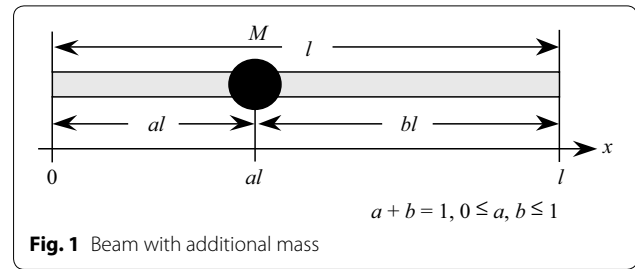
$$f_n = \frac{1}{2\pi} \left(\frac{m_n}{l} \right)^2 \sqrt{\frac{EI}{\rho A}}. \tag{3}$$

From Eqs. (1) and (3),

$$m_n = \sqrt{\frac{f_n}{f_{n0}}} m_{n0}. \tag{4}$$

The frequency equation for the free–free vibration with the concentrated mass M placed at position $x = al$ (x: distance along the bar, $0 \leq a \leq 1$, $a + b = 1$) on a bar (Fig. 1) is expressed as follows:

Fig. 1 Beam with additional mass

where μ is the ratio of the concentrated mass to the mass of the bar and is defined as

$$\mu = \frac{M}{\rho A l}. \tag{6}$$

The measured resonance frequencies f_{n0} and f_n are substituted into Eq. (4) to calculate m_n, and the calculated m_n is substituted into Eq. (5) to calculate μ. The specimen mass and density can be obtained by substituting the calculated μ, the concentrated mass, and the dimensions of a bar into Eq. (6). Young's modulus can be calculated by substituting the estimated density, the resonance frequency without the concentrated mass, and the dimensions of a bar into Eq. (1) [1–6].

The above steps represent the calculation procedure for the VAM. Weighing the specimen is not required for the calculations.

Goens–Hearmon regression method based on the Timoshenko theory of bending (TGH method)

Young's and shear moduli can be obtained simultaneously using only the bending vibration test without a torsional vibration test by the following the Goens–Hearmon regression method based on the Timoshenko theory of bending (TGH method) [13–15].

The apparent deflection in the bending vibration consists of deflections due to shear and rotatory inertia, as well as pure bending deflection. Timoshenko added the terms deflections of shear and rotatory inertia to the Euler–Bernoulli elementary theory of bending and developed the following differential equation of bending [13]:

$$(\cos m_n \cosh m_n - 1) - \frac{1}{2}\mu m_n \{ (\cos a m_n \cosh a m_n + 1)(\sin b m_n \cosh b m_n - \cos b m_n \sinh b m_n) \\ + (\cos b m_n \cosh b m_n + 1)(\sin a m_n \cosh a m_n - \cos a m_n \sinh a m_n) \} = 0, \tag{5}$$

$$\frac{EI}{\rho A}\frac{\partial^4 y}{\partial x^4} + \frac{\partial^2 y}{\partial t^2} - \frac{I}{A}\left(1 + \frac{sE}{G}\right)\frac{\partial^4 y}{\partial x^2 \partial t^2} + \frac{\rho sI}{GA}\frac{\partial^4 y}{\partial t^4} = 0, \tag{7}$$

where G is the shear modulus, y is the lateral deflection, and t is the time.

When Eq. (7) is solved under the free–free condition, the resonance frequency corresponding to the nth mode f_{gn0} can be written as follows:

$$f_{gn0} = \frac{1}{2\pi}\left(\frac{k_{n0}}{l}\right)^2\sqrt{\frac{EI}{\rho A}} = \frac{1}{2\pi}\left(\frac{m_{n0}}{l}\right)^2\sqrt{\frac{E_{an}I}{\rho A}}, \tag{8}$$

where E_{an} is Young's modulus from the Euler–Bernoulli elementary theory of bending using the resonance frequency of the nth mode.

k_{n0} in Eq. (8) is obtained by transcendental equations represented as follows:

$$\frac{\tan\frac{k_{n0}}{2}\sqrt{\sqrt{B_t^2 k_{n0}^4 + 1} + A_t k_{n0}^2}}{\tanh\frac{k_{n0}}{2}\sqrt{\sqrt{B_t^2 k_{n0}^4 + 1} - A_t k_{n0}^2}} = -\frac{\sqrt{\sqrt{B_t^2 k_{n0}^4 + 1} + A_t k_{n0}^2}}{\sqrt{\sqrt{B_t^2 k_{n0}^4 + 1} - A_t k_{n0}^2}}\frac{\sqrt{B_t^2 k_{n0}^4 + 1} - B_t k_{n0}^2}{\sqrt{B_t^2 k_{n0}^4 + 1} + B_t k_{n0}^2} \text{ (for symmetric modes),} \tag{9}$$

and

$$\frac{\cot\frac{k_{n0}}{2}\sqrt{\sqrt{B_t^2 k_{n0}^4 + 1} + A_t k_{n0}^2}}{\coth\frac{k_{n0}}{2}\sqrt{\sqrt{B_t^2 k_{n0}^4 + 1} - A_t k_{n0}^2}} = +\frac{\sqrt{\sqrt{B_t^2 k_{n0}^4 + 1} + A_t k_{n0}^2}}{\sqrt{\sqrt{B_t^2 k_{n0}^4 + 1} - A_t k_{n0}^2}}\frac{\sqrt{B_t^2 k_{n0}^4 + 1} - B_t k_{n0}^2}{\sqrt{B_t^2 k_{n0}^4 + 1} + B_t k_{n0}^2} \text{ (for asymmetric modes),} \tag{10}$$

where

$$A_t = \frac{I}{2l^2 A}\left(1 + \frac{sE}{G}\right), \tag{11}$$

and

$$B_t = \frac{I}{2l^2 A}\left(-1 + \frac{sE}{G}\right). \tag{12}$$

Goens approximated Eqs. (9) and (10) using a Taylor series into the following formula [14]:

$$\frac{m_{n0}^4}{k_{n0}^4} = \frac{E}{E_{an}} = T = 1 + \frac{I}{l^2 A}\left\{m_{n0}^2 F^2(m_{n0}) + 6m_{n0}F(m_{n0})\right\} + \frac{I}{l^2 A}\frac{sE}{G}\left\{m_{n0}^2 F^2(m_{n0}) - 2m_{n0}F(m_{n0})\right\} - \frac{4\pi^2\rho sIf_{n0}^2}{GA}, \tag{13}$$

where

$$F(m_{10}) = 0.9825, F(m_{20}) = 1.0008, F(m_{n0}) = 1(n > 2). \tag{14}$$

Approximately,

$$T = 1 + \frac{I}{l^2 A}\left[\left\{m_{n0}^2 F^2(m_{n0}) + 6m_{n0}F(m_{n0})\right\} + \frac{sE}{G}\left\{m_{n0}^2 F^2(m_{n0}) - 2m_{n0}F(m_{n0})\right\}\right]. \tag{15}$$

Hearmon calculated E and G using the following procedure after separating Eq. (13) as follows [15]:

$$Y = E_{an}\left[1 + \frac{I}{l^2 A}\left\{m_{n0}^2 F^2(m_{n0}) + 6m_{n0}F(m_{n0})\right\} - \frac{4\pi^2\rho sIf_{n0}^2}{GA}\right], \tag{16}$$

$$X = E_{an}\frac{I}{l^2 A}\left\{m_{n0}^2 F^2(m_{n0}) - 2m_{n0}F(m_{n0})\right\}, \tag{17}$$

$$\alpha = \frac{sE}{G}, \tag{18}$$

$$\beta = E, \tag{19}$$

and then from Eqs. (16)–(19):

$$Y = -\alpha X + \beta. \tag{20}$$

Therefore, the linear regression between X and Y provides the E and G values. This is the Goens–Hearmon regression method based on the Timoshenko theory of

Kubojima *et al. J Wood Sci* (2020) 66:51

Page 4 of 8

bending (TGH method). The value of *s* is 6/5 theoretically [16] and 1.18 experimentally [17] for the rectangular cross section and 10/9 [16] for the circular cross section.

Materials and methods

Specimens

Sitka spruce (*Picea sitchensis* Carr.) rectangular bars with a width of 30 mm (radial direction, R), thicknesses of 5, 10, 15, 20, 25, 30, 35, 40, 45, 50, 55, and 60 mm (tangential direction, T), and a length of 300 mm (longitudinal direction, L) were used as the specimens. Japanese cedar (*Cryptomeria japonica* D. Don) small round bars without a pith with varying diameters of 6, 9, 20, 25, 30, and 36 mm and a length of 300 mm, and those with a diameter of 36 mm and varying lengths of 150, 200, and 250 mm were used as the specimens. Three specimens were made for each dimension. Three Japanese cedar cross beams for timber guardrails with a pith having a diameter of 200 mm and a length of 1980 mm [11] were also used as the specimens. Considering the variation in the results of the vibration test, the number of specimens was three.

The specimens were conditioned at 20 °C and 65% relative humidity. All tests were conducted under the same conditions.

Vibration tests

Free–free bending vibration tests were conducted to measure the resonance frequencies of the first to fifth resonance modes using the following procedure: the test bar without a concentrated mass was suspended by two threads at the nodal positions of the free–free vibration, corresponding to each resonance mode. The bending vibration was subsequently generated by tapping the LR-plane of the rectangular bars and the small round bars in the T-direction and it was generated by tapping the LT-plane of the cross beams for timber guardrails in the R-direction, using a wooden hammer. The motion of the specimen was detected with a microphone. The signal was processed through a fast Fourier transform (FFT) digital signal analyzer (Multi-Purpose FFT Analyzer CF-5220, Ono-Sokki, Co., Ltd., Yokohama, Japan) to yield the high-resolution resonance frequencies. A diagram of the experimental setup is provided in Fig. 2.

The free–free bending vibration tests were also performed on the specimens with the concentrated mass using the procedure described above and the resonance frequency of the first mode was measured. Iron plates, thumbtacks, and wood screws were used as the concentrated mass. The position of the concentrated mass was $x = 0.5\ l$, considering the on-site quality evaluation of cross beams of wooden guardrails. The concentrated masses and specimens are shown in Tables 1 and 2.

Results and discussion

The mean (standard deviation) density and Young's modulus of the specimens were 449 (14) kg/m^3, 14.23 (0.45) GPa (sitka spruce rectangular bars; TGH method), and 351 (16) kg/m^3, 10.05 (1.04) GPa (Japanese cedar small round bars; TGH method), respectively.

The estimation accuracy of the VAM, which is expressed by the mass ratio (estimated specimen mass through the VAM/measured specimen mass), increased as the length/thickness ratio of the rectangular bar and the length/diameter ratio of the small round bar increased, as shown in Fig. 3. Conversely, the effect of deflections due to shear and

Fig. 2 Schematic diagram of the experimental setup for the bending vibration tests
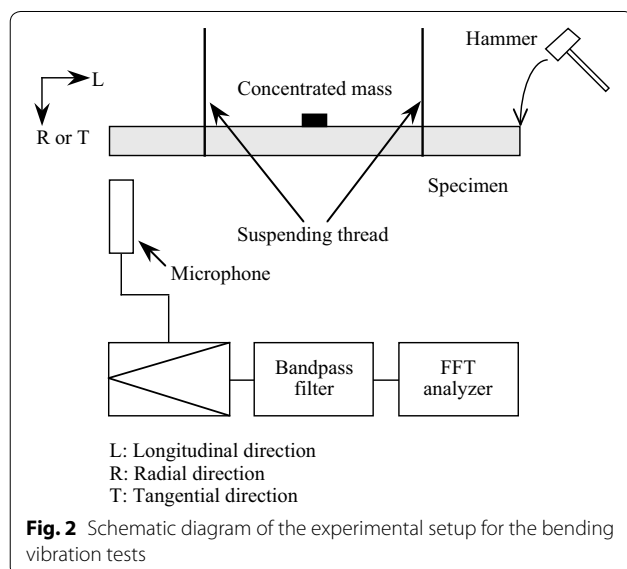
Table 1 Concentrated masses (iron plates) attached to rectangular bars

Concentrated mass		Specimens	Mass ratio μ
Dimensions	Mass	Dimensions	
2 × 2 × 30	1.0	30 × 5 × 300	0.0453
4 × 2 × 30	2.0	30 × 10 × 300	0.0474
7 × 2 × 30	3.2	30 × 15 × 300	0.0504
9 × 2 × 30	4.1	30 × 20 × 300	0.0492
11 × 2 × 30	5.1	30 × 25 × 300	0.0524
13 × 2 × 30	6.0	30 × 30 × 300	0.0518
14 × 2 × 30	7.0	30 × 35 × 300	0.0512
17 × 2 × 30	7.9	30 × 40 × 300	0.0506
20 × 2 × 30	9.4	30 × 45 × 300	0.0515
21 × 2 × 30	10.3	30 × 50 × 300	0.0510
24 × 2 × 30	11.3	30 × 55 × 300	0.0506
26 × 2 × 30	12.2	30 × 60 × 300	0.0507

Unit of dimensions: mm, unit of mass: g

Kubojima *et al. J Wood Sci*   (2020) 66:51

Page 5 of 8

Table 2 Concentrated masses (thumbtacks, wood screws) attached to small round bars

Concentrated mass					Specimens	Mass ratio μ
Type	Head diameter	Nominal diameter	Length	Mass	Diameter, length	
Thumbtack	11	1	8	0.6	6, 300	0.214
					9, 300	0.0905
Wood screw	6	4	32	2.1	20, 300	0.0615
					25, 300	0.0437
					36, 150	0.0393
Wood screw	9	5	37	3.6	30, 300	0.0503
					36, 200	0.0485
					36, 250	0.0395
Wood screw	8	4	65	3.9	36, 300	0.0392

Units of diameter and length: mm, unit of mass: g
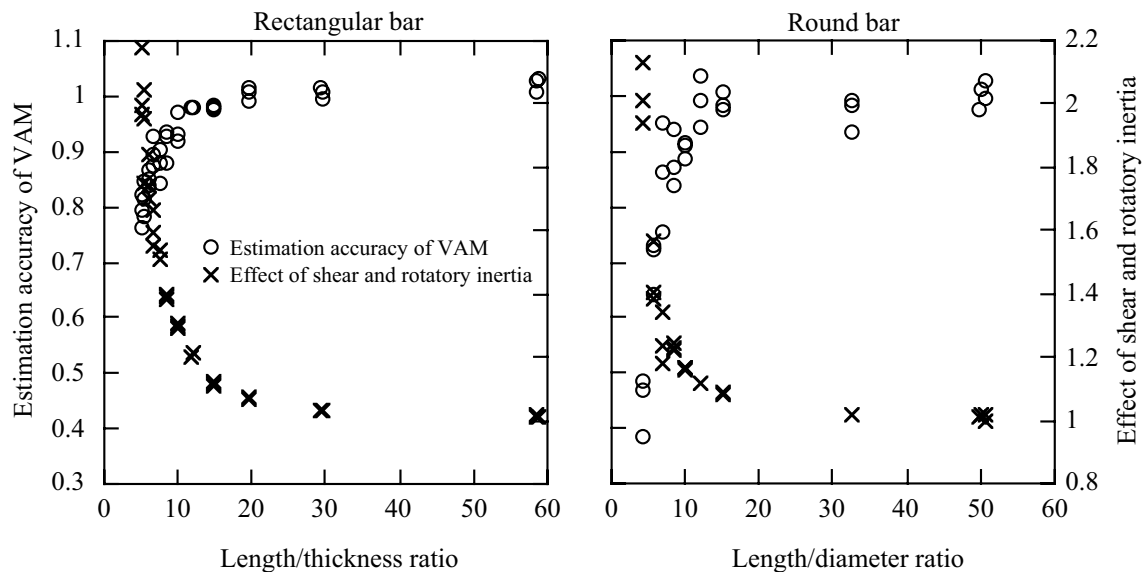
Fig. 3 Estimation accuracy of the VAM and the effect of deflections due to shear and rotatory inertia involved in the bending vibrational deflection (SR effect) at various length/thickness and length/diameter ratios

rotatory inertia involved in the bending vibration deflection (SR effect) shown by T (E_{an} is calculated from the first resonance mode in this study) in Eq. (13) decreased as the length/thickness and length/diameter ratios increased, as shown in Fig. 3. Thus, the estimation accuracy of the VAM is discussed from the aspect of T.

When the SR effect is taken into consideration, the resonance frequency without the concentrated mass is expressed by Eq. (8), and the resonance frequency with the concentrated mass is expressed as follows:

$$f_{gn} = \frac{1}{2\pi} \left(\frac{k_n}{l} \right)^2 \sqrt{\frac{EI}{\rho A}}. \tag{21}$$

From Eqs. (8) and (21),

$$k_n = \sqrt{\frac{f_{gn}}{f_{gn0}}} k_{n0} = \sqrt{\frac{f_{gn}}{f_{gn0}}} \frac{m_{n0}}{\sqrt[4]{T}}. \tag{22}$$

When the SR effect can be ignored, the m_n decreases monotonically with μ for the free–free vibration [5]. Hence, the specimen mass estimated by the VAM is low for a low m_n from Eq. (6). Analogizing this, when k_n decreases, μ increases, and the specimen mass decreases, which causes the estimation accuracy of the VAM to decrease. Equation (22) shows that k_n decreases with an increasing T. Therefore, when T increases with the decreases in the length/thickness and length/diameter ratios, k_n decreases, causing the estimation accuracy of the VAM to decrease.

Kubojima *et al. J Wood Sci* (2020) 66:51

Page 6 of 8

As the SR effect is not taken into consideration in Eq. (5), k_n cannot be directly substituted for Eq. (5). In other words, f_n/f_{n0} needed to be used instead of f_{gn}/f_{gn0} for Eq. (4). With the assumption that the SR effect changes f_n/f_{n0} to f_{gn}/f_{gn0}, the relationship between $(f_{gn}/f_{gn0})/(f_n/f_{n0})$ and T was investigated. For this purpose, $(f_{gn}/f_{gn0})/(f_n/f_{n0})$ was plotted against T. m_n was calculated by substituting μ, which is the ratio of the measured concentrated mass to the specimen mass, for Eq. (5), and f_n/f_{n0} was then obtained from Eqs. (2) and (4). Mathematica (version 10.4 J, Wolfram Research Co., Ltd.) was used for solving Eq. (5). $(f_{gn}/f_{gn0})/(f_n/f_{n0})$ (f_{gn} and f_{gn0} are measured values) linearly decreased with an increasing T, as shown in Fig. 4 and the regression equations of Eqs. (23) and (24) were obtained:

$$\frac{f_{gn}/f_{gn0}}{f_n/f_{n0}} = -0.0084T + 1.01 \left(r = 0.972^{**}, n = 1 \right) \text{for the rectangular bar,} \tag{23}$$

$$\frac{f_{gn}/f_{gn0}}{f_n/f_{n0}} = -0.030T + 1.03 \left(r = 0.956^{**}, n = 1 \right) \text{for the small round bar.} \tag{24}$$

The estimation accuracy of the VAM is corrected with the following method. f_n/f_{n0} was estimated by substituting the measured $T = E/E_{an}$ (TGH method/Euler–Bernoulli elementary theory) and measured f_{gn}/f_{gn0} for Eqs. (23) and (24). The estimated f_n/f_{n0} was used for Eq. (4), and

m_n was subsequently obtained. The specimen mass was estimated by substituting the obtained m_n for Eq. (5). The results showed that the estimation accuracy of the VAM was improved, as shown in Fig. 5. The estimation accuracy of the VAM could not be improved in several cases. In such cases, $(f_{gn}/f_{gn0})/(f_n/f_{n0})$ was out of lines that are shown by Fig. 4 and Eqs. (23) and (24).

As mentioned above, $T = E/E_{an}$ is necessary to estimate f_n/f_{n0} from f_{gn}/f_{gn0}. In other words, the bending Young's modulus based on the Euler–Bernoulli elementary theory, which can be calculated by measuring one resonance mode, and the "true" Young's modulus without the SR effect are required. The true Young's modulus can be measured through the TGH method or the longitudinal vibration test. As the resonance frequencies of plural vibration modes are required, obtaining $T = E/E_{an}$ on-site, where simplicity and speed are needed, is challenging.

Since the estimation accuracy of the VAM was high when T was small, as shown in Fig. 3, T that provides a sufficiently high estimation accuracy of VAM is discussed
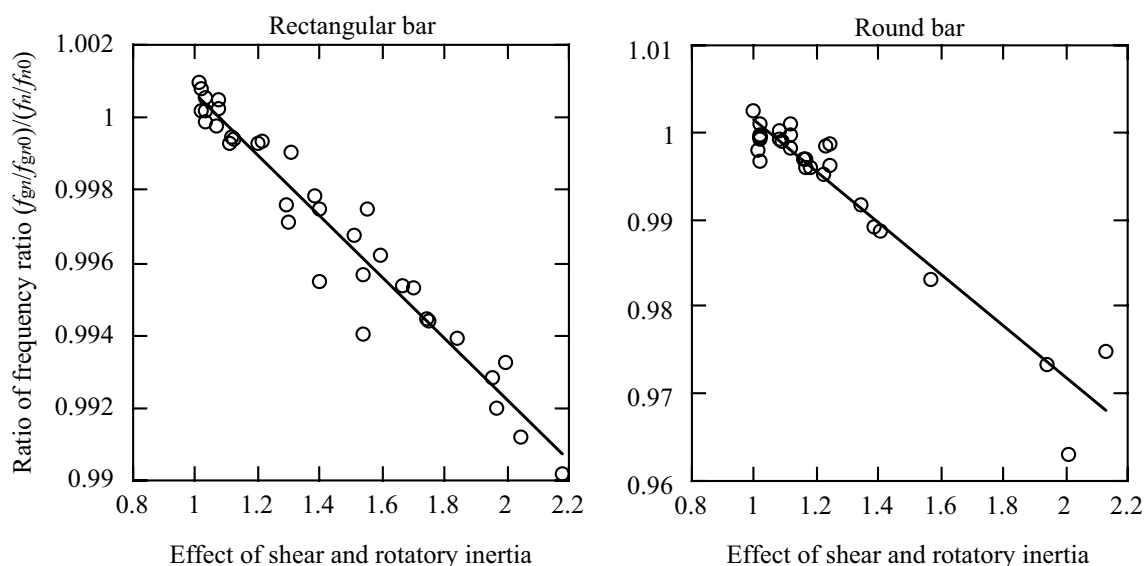
Fig. 4 Relationship between the ratio of frequency ratio $(f_{gr}/f_{gn0})/(f_n/f_{n0})$ and the effect of deflections due to shear and rotatory inertia involved in the bending vibrational deflection T

Kubojima *et al. J Wood Sci* (2020) 66:51

Page 7 of 8
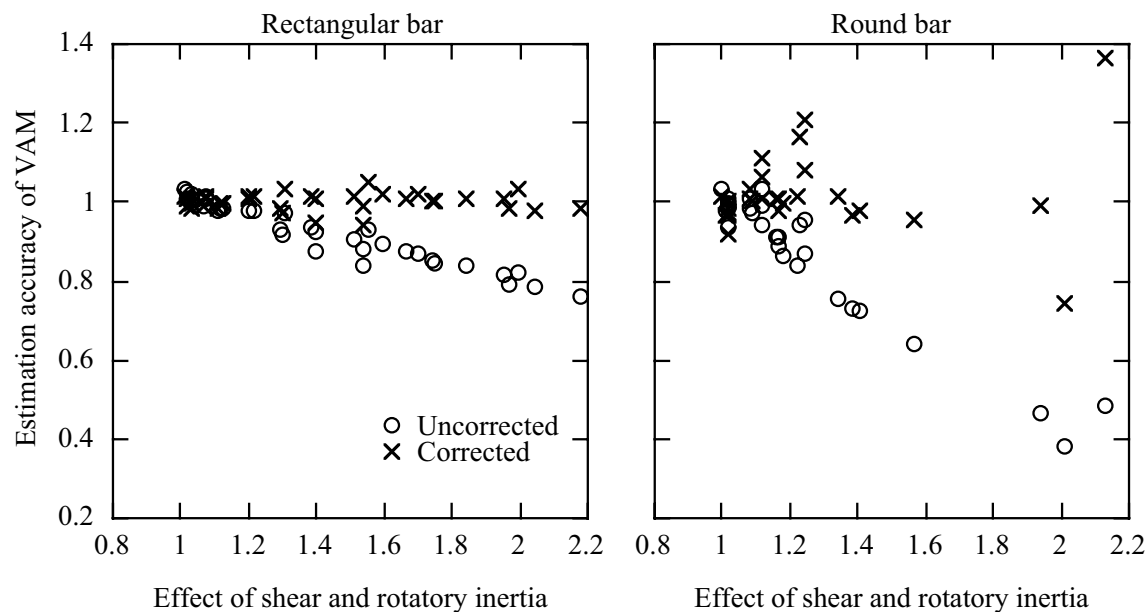
Fig. 5 Relationship between the estimation accuracy of the VAM and the effect of deflections due to shear and rotatory inertia involved in the bending vibrational deflection T

here. Based on the coefficient of regression of the TGH method in our previous study, the SR effect was experimentally low in the range of $T \leq 1.2$ [18]. In the range of $T \leq 1.2$, the estimation accuracy of the VAM for 11 out of 11 specimens (100%) for rectangular bars and that for 15 out of 17 specimens (88%) for small round bars were from 0.9 to 1.1. Hence, it can be said that the estimation accuracy of the VAM is sufficiently high in the range of $T \leq 1.2$. The estimation accuracies of the VAM for cross beams of wooden guardrails were 0.89, 0.91, and 1.06 [11] for $T = 1.13$, 1.11, and 1.17, respectively. The dimensions of a specimen that give $T \leq 1.2$ can be calculated by substituting $T = 1.2$, Young's modulus and shear modulus published in the literature for Eq. (15).

Conclusions

Bending vibrations were undertaken for rectangular bars and round bars with various dimensions with and without the concentrated mass, and the following results were obtained:

1. The estimation accuracy of the VAM and the SR effect increased and decreased, respectively, as the length/thickness ratio of the rectangular bar and the length/diameter ratio of the round bar increased.
2. The estimation accuracy of the VAM decreased as the SR effect increased.
3. The SR effect on the estimation accuracy of the VAM could be corrected.

4. The range of T for obtaining a sufficiently high accuracy of VAM was $T \leq 1.2$.

Author details
[1] Forestry and Forest Products Research Institute, 1 Matsunosato, Tsukuba, Ibaraki 305-8687, Japan. [2] Toyama Prefectural Agricultural, Forestry & Fisheries Research Center, 4940 Kurokawa Shin, Imizu, Toyama 939-0311, Japan.

Kubojima *et al. J Wood Sci*   (2020) 66:51

Page 8 of 8

References

1. Skrinar M (2002) On elastic beams parameter identification using eigen-frequencies changes and the method of added mass. Comput Mater Sci 25:207–217
2. Türker T, Bayraktar A (2008) Structural parameter identification of fixed end beams by inverse method using measured natural frequencies. Shock Vib 15:505–515
3. Kubojima Y, Sonoda S (2015) Measuring Young's modulus of a wooden bar using longitudinal vibration without measuring its weight. Eur J Wood Wood Prod 73:399–401
4. Matsubara M, Aono A, Kawamura S (2015) Experimental identification of structural properties of elastic beam with homogeneous and uniform cross section. Trans JSME. https://doi.org/10.1299/transjsme.15-00279
5. Kubojima Y, Kato H, Tonosaki M, Sonoda S (2016) Measuring Young's modulus of a wooden bar using flexural vibration without measuring its weight. BioResources 11:800–810
6. Matsubara M, Aono A, Ise T, Kawamura S (2016) Study on identification method of line density of the elastic beam under unknown boundary conditions. Trans JSME. https://doi.org/10.1299/transjsme.15-00669
7. Sonoda S, Kubojima Y, Kato H (2016) Practical techniques for the vibration method with additional mass. Part 2: experimental study on the additional mass in longitudinal vibration test for timber measurement. In: CD-ROM proceedings of the world conference on timber engineering (WCTE 2016), Vienna, Austria, August 22–25, 2016
8. Kubojima Y, Sonoda S, Kato H (2017) Practical techniques for the vibration method with additional mass: effect of crossers' position in longitudinal vibration. J Wood Sci 63:147–153
9. Kubojima Y, Sonoda S, Kato H (2017) Practical techniques for the vibration method with additional mass: effect of specimen moisture content. J Wood Sci 63:568–574
10. Kubojima Y, Sonoda S, Kato H (2018) Practical techniques for the vibration method with additional mass: bending vibration generated by tapping cross section. J Wood Sci 64:16–22
11. Kubojima Y, Sonoda S, Kato H (2018) Application of the vibration method with additional mass to timber guardrail beams. J Wood Sci 64:767–775
12. Kubojima Y, Sonoda S, Kato H (2020) Mass of piled lumber estimated through vibration test. J Wood Sci 66:32. https://doi.org/10.1186/s10086-020-01880-5
13. Timoshenko SP (1921) On the correction for shear of the differential equation for transverse vibrations of prismatic bars. Philos Mag 6 Ser 41(245):744–746
14. Goens E (1931) Über die Bestimmung des Elastizitätsmodulus von Stäben mit Hilfe von Biegungsschwingungen. Ann Phys 403(6):649–678
15. Hearmon RFS (1958) The influence of shear and rotatory inertia on the free flexural vibration of wooden beams. Br J Appl Phys 9(10):381–388
16. Timoshenko SP, Gere JM (1972) Mechanics of materials. D. Van Nostrand Company, New York
17. Nakao T, Okano T, Asano I (1984) Measurement of anisotropic shear modulus by the tortional-vibration method for free–free wooden beams. Mokuzai Gakkaishi 30:877–885
18. Kubojima Y, Yoshihara H, Ohta M, Okano T (1996) Examination of the method of measuring the shear modulus of wood based on the Timoshenko theory of bending. Mokuzai Gakkaishi 42:1170–1176

Publisher's Note